

Optical microflow cytometer for particle counting, sizing and fluorescence detection

Han-Taw Chen · Yao-Nan Wang

Received: 27 May 2008 / Accepted: 17 July 2008 / Published online: 6 August 2008
© Springer-Verlag 2008

Abstract A novel on-chip optical flow cytometer concept is reported for fluorescence detection, enumeration, and sizing of microparticles in a poly-dimethylsiloxane (PDMS) microchip. The detection system integrates a pair of external optical fibers and other optical components for particle counting, sizing and fluorescence analysis in each measurement simultaneously. The scattered light signal indicates the total number and the size of the particles passing through the detection window, whereas the concurrent backward fluorescence signal shows only the number of fluorescence particles. In the experiments, microparticles of four different sizes with diameters ranging from 3.2 to 10.2 μm were discriminated and counted based on the fluorescence and scattered light intensity. The relative percentage of the fluorescence-labeled particles can be analyzed by the ratio of the events of fluorescence signals to forward scattered signals.

Keywords Microchip · Microflow cytometer · Microfluidic · PDMS

1 Introduction

Flow cytometry has been a versatile tool with extensive applications in biomedical research, diagnosis, and therapy for cell counting and sorting in clinical laboratories by optical means. It offers a practical solution for satisfying the detection tasks and therefore requires specific lasers to excite samples for generating different wavelengths. This

method integrates multiplex forward scatter and side scatter for simultaneous sizing and specific biomarker identification when a particle or cell passes through the detection region (Haynes John 1988; Scott Cram 2002). Commercial benchtop flow cytometers have high performance and sensitivity. However, the expensive cost is a major obstacle for most research laboratories. With the development of microfluidic systems, microflow cytometry provides an excellent detection platform to achieve lower sample consumption and produces inexpensive alternative instruments for bioparticle sizing and fluorescence analysis.

In the past decade, a number of microflow cytometers have been developed incorporating microfabrication technologies and small components to miniaturize the devices for bioparticle detection based on different techniques. The development of microflow cytometer has been recently described in some comprehensive review papers (Erickson and Li 2004; Mogensen et al. 2004; Huh et al. 2005; Yi et al. 2006; Ateya et al. 2008). The Coulter counter is the first flow cytometer. It is a classic flow cytometer based on the electronic detection method that employs the modulation of electrical resistance in an electrical ion current for label-free biological sample identification and analysis. Resistive pulse sensing method has been widely applied for sensing microparticles, such as polystyrene particles (Xu et al. 2007), single DNA molecules (Saleh and Sohn 2003a), proteins (Wharton et al. 2007), antigen and antibody (Saleh and Sohn 2003b; Carbonaro and Sohn 2005). The sensitivity of resistive pulse approach depends on the volume ratio of the sample and has a much lower manufacturing and operational cost. Electrical microimpedance measurements (Cheung et al. 2005; Sun et al. 2007; Rodriguez-Trujillo et al. 2007) can extract the cells/particles size information from the sensing microelectrodes

H.-T. Chen (✉) · Y.-N. Wang
Department of Mechanical Engineering,
National Cheng-Kung University, Tainan 701, Taiwan
e-mail: htchen@mail.ncku.edu.tw

fabricated on different substrates by microfabrication technology. Multi-aperture Coulter counter (Jagtiani et al. 2006; Zhe et al. 2007) integrated more sensing channels and improved the counting efficiency and throughput.

For the particle counting and sizing, the other method is a fluorescent optical scheme based on light scattering techniques (Pamme et al. 2003; Wang et al. 2004) and laser-induced fluorescence techniques (Chen and Wang 2008; Dittrich and Schwille 2003; Fu et al. 2004). Some researchers (Dittrich and Schwille 2003; Fu et al. 2008; Huh et al. 2002; Knittle et al. 2007; Luo et al. 2005; McClain et al. 2001; Yao et al. 2004) have integrated a fluorescent microscope with a high sensitivity photodetector for bioparticle counting and sorting. However, an alternative approach for fluorescence detection is to use micromachining processes to integrate fibers as a waveguide (Bernini et al. 2006; Cui et al. 2002; Fu et al. 2004; Xiang et al. 2005; Tung et al. 2004) on the microchip, shortening the optical path and increasing the detection efficiency. This approach utilizes embedded fibers and an integrated microscope and are therefore have limited use for complex manufacturing processes and bulky equipment. The detection systems mentioned above provide information for either sizing or fluorescence identification only.

To realize commercial flow cytometer concepts for sizing and fluorescence detection simultaneously on a microchip, Morgan et al. (2006) integrated a fluorescence microscope system, photomultiplier tube (PMT) and microfabricated electrodes on a microchip for single-particle fluorescence spectroscopy and multi-frequency electrical impedance analysis simultaneously. Two pairs of metal electrodes were fabricated at the bottom of a microchannel along either side of the detection window for dielectrophoretic focusing, and the laser beam was focused at the mid-height of the channel for fluorescence detection. When a fluorescence particle passes through the detection window, the particles of different sizes can be discriminated by both fluorescent intensity and AC impedance signal amplitude. In a recent paper, the authors (Wang et al. 2008) demonstrated a flow cytometer-like concept on a microfluidic chip for CD4+ T lymphocytes counting and fluorescence detection based on the MOSFET-enhanced Coulter counter and laser-induced fluorescence technique. The exciting laser light was focused underneath the detection region of coulter counter on the microchip. The MOSFET signal indicates the total number of the cells passing through the detection channel, while the concurrent fluorescence signal shows only the number of cells tagged with a specific fluorescent dye. The absolute count and the relative percentage of the CD4+ T cells can be analyzed accurately by combining both results. Both the above hybrid systems use the electrical method for total particle

counting and the optical method for fluorescence enumeration.

In this paper, a novel and reliable on-chip optical flow cytometer was demonstrated that integrates fluorescence and light scattering measurement for simultaneous particle counting, sizing and fluorescence detection. A pair of external fibers was placed in coaxial alignment on a polydimethylsiloxane (PDMS) microchip composed of a thin glass substrate and PDMS microchannel. One fiber is for transmittal of both excitation laser light and fluorescence emission light of the particle, while the other one is for particle scatter light detection concurrently. The sizing and total count of the particles are decided based on the forward scattered signals, and the count of fluorescence particles can be decided based on the backward fluorescence signal. The total counting, size discrimination and relative percentage of the fluorescence particles can be analyzed by combining both results.

2 Materials and methods

2.1 Measurement of fluorescent and non-fluorescent beads

When compared with actual cells, the commercial flow cytometer calibration polystyrene particles are easily available and have standard size distribution. Therefore, in this proof of concept experiment, polystyrene microparticles of five different sizes were used to evaluate the performance of the proposed microfluidic system. The ultra rainbow fluorescent particles of a mean diameter of 10.2 μm (8.1–12 μm ; Bangs Laboratories Inc.) with a concentration of 2×10^6 beads/ml were originally supplied as a suspension in deionized water of 0.02% sodium azide and 0.01% NP40. Rainbow fluorescent particles 3.0–3.4 μm (BD Biosciences) have a concentration of 2×10^6 beads/ml. The 9.86 μm diameter non-fluorescent particles (F13838, Invitrogen, Carlsbad, CA, USA) were placed in distilled water with 0.05% Tween 20 and 2 mM sodium azide. The non-fluorescence 6 μm diameter particles (Molecular Probe) and 4.8 μm polystyrene beads (Bangs Laboratories Inc.) both have a concentration of 2×10^7 beads/ml. All the particles were re-suspended into appropriate concentrations using 7.5 mM sodium boric buffer (with a pH value of 9.39) before the test in 1 ml aliquots.

2.2 Microchip fabrication

In the microchip fabrication process, the mold masters containing the convergent microchannel patterns were made by spin coating SU-8 2075 photoresist on a clean glass slide at 2,000 rpm. After soft baking at 65°C for 5 min

and 95°C for 15 min, the photoresist film was exposed to UV light for 6 s using a 12,000 dpi photomask on which the desired channel pattern was printed. Following hard baking at 65°C for 1 min and 95°C for 4 min, the slide was put into a SU-8 developer and was slightly agitated until the master was fully developed. The master was rinsed with DI water on both sides and was hard baked at 250°C for 20 min. A mixture of Sylgard 184 (Dow Corning, MI, USA) and its curing agent with the ratio of 10:1, by weight, was poured over the master and degassed in a vacuum oven (25 in. Hg) for 1 h followed by a curing at 75°C for another 3–4 h. The PDMS cast with the microchannel pattern was then carefully peeled off from the master. A hole was punched on each side of the microfluidic channel to form the well for injection of sample solution. The PDMS cast and a piece of cleaned thin glass slide were then treated in a plasma discharger (PDC-32G, Harrick Scientific, USA) for 30 s, the PDMS was then cast and a clean glass slide were bonded.

2.3 Experimental setup

Figure 1a shows the structure of the optical flow cytometer system. The optical detection system operation mechanism is similar to the conventional flow cytometer in that a laser beam is used as the excitation source and the forward scattered light is used for particle size discrimination. However, different from the conventional methods, the backward fluorescence light takes place of the side scattered light for fluorescence detection in this device. The microchip was assembled with a PDMS on a glass substrate (24 × 60 × 0.15 mm, VWR International). Figure 1b shows the dimensions of microchannel that consists of a main channel of 200 μm in width and 30 μm in depth, and 50 μm in width and 200 μm in length for the detection gate. The detection gate channel is connected to the main channel through two convergent sections for the passive focusing of the particles. Before each test, the channel and wells were primed with 7.5 mM of sodium borate buffer. The particle suspension was introduced into a reservoir and electroosmotic flow was induced in the horizontal channel by applied voltage bias to the ends of main channel to drive sample through the channel.

The microchip and the relative location of detection fiber arrange between XYZ 3-axis travel translation stage and XY translator as shown in Fig. 1c. The microchip was mounted horizontally on a hollow metal platform. A pair of optical fibers (NA of 0.22, 50 and 200 μm in diameter, Silicon Lightwave Technology, CA, USA) was fixed on a movable cartridge which was installed on both sides of the microchip in the opposite position. The open tip of the optical fibers was in coaxial arrangement in the vertical direction orthogonally opposing the upstream end of the microchip convergent channel. The 200 μm optical fiber

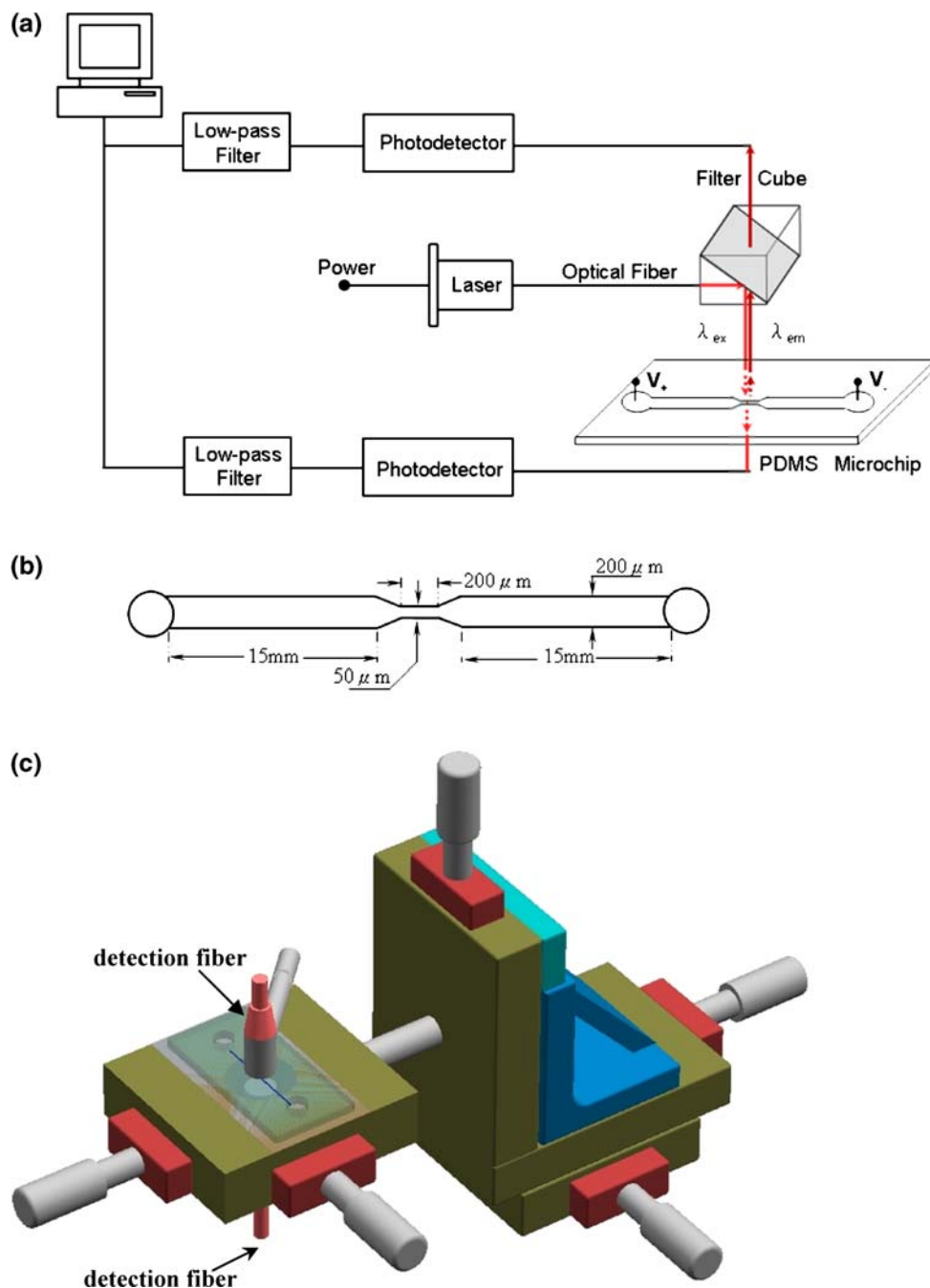
was mounted on the top of the microchip for transmission of laser excitation light and for the collection of the fluorescence light. The 50 μm optical fiber was mounted on the bottom of the microchip for collection of the scattered light. The fluorescence signal denotes the labeled particles passing through the detection region and the scattered light intensity denotes the particle sizing and counting. The precise alignment between the microchip detection region and the sizing optical fiber was achieved by an XYZ 3-axis travel translation stage and XY translator (Thorlabs, Newton, NJ, USA). An optical microscope (SMZ800, Nikon Instrument Inc.) and a CCD camera (Qimaging, Vancouver, BC, Canada) were used to monitor the alignment of the scattering light fiber. In the two fiber alignment, the baseline was in the highest level when the laser source fiber and scattering detection fiber were arranged in the coaxial direction. The microchip of the convergent channel was clapped in a sandwich-like configuration between two detection fibers. The core of the optical fiber can cover the whole channel to detect the particles when particles pass through the detection channel.

2.4 Fluorescence detection and scattered light counting

For the laser-induced fluorescence detection, the 200 μm optical fiber was fixed in a movable cartridge on top of the microchip to transmit excitation laser light and to receive fluorescence emission light. The excitation was done by a 25-mW single-mode diode laser (wavelength of 635 nm, Blue Sky Research, CA, USA) coupled with fiber. The laser beam went through a filter cube (OZ Optics, Canada) and was reflected into the fluorescence detecting fiber by the dichroic mirror. The laser beam was focused at the convergent channel by the fluorescence detection fiber that transmitted both excitation laser light and sample emission light concurrently. In the microflow cytometer microchip, both the glass substrate and PDMS microchip are transparent so that the optical detection window is capable of transmitting optical signals in the interrogation region. The schematic diagram outlining the principle of the system and cross-sectional dimensions of the microchip were shown in Fig. 2. The two detection fibers were externally in contact with the top and bottom of the microchip. The distance between the two optic fibers is 1,150 μm. The distance from scattered light detection fiber to the particles is less than 180 μm.

For particle size measurement, the external fiber works as a waveguide for the incident excitation laser which is focused on the detection region. Forward scattered light transmitting the detection window is collected through the 50 μm scattering detection fiber opposite to the excitation fiber. Therefore, the scattered intensity signal is kept at a stable level when the scattering detection fiber receives

Fig. 1 **a** Schematics of the system setup. **b** Dimensions of the microchannel. **c** Schematic layout of detection fiber, XYZ 3-axis travel translation stage and XY translator



direct incident light. When particles pass through the detection window, the particle scatters the incident light. The change of the incident light intensity will be received and recorded through the opposite scattering light detection fiber. When a fluorescent particle passes through the detection area, the fluorescent tag is excited. The emission light is backward transmitted by the fiber pass through dichroic mirror and a band pass filter and then recorded by the photo-detector.

The optical signals were translated into electric signal by avalanche photo-detector (C5460-01, Hamamatsu,

Japan). The signal recording and analysis were performed by a custom-made LABVIEW[®] code through a data acquisition board (PCI 6281, National Instruments, Austin, TX, USA).

3 Results and discussion

In this study, the performance of the proposed cytometer was investigated using 100% fluorescent particles. As shown in Fig. 3, the typical forward scattered signal and

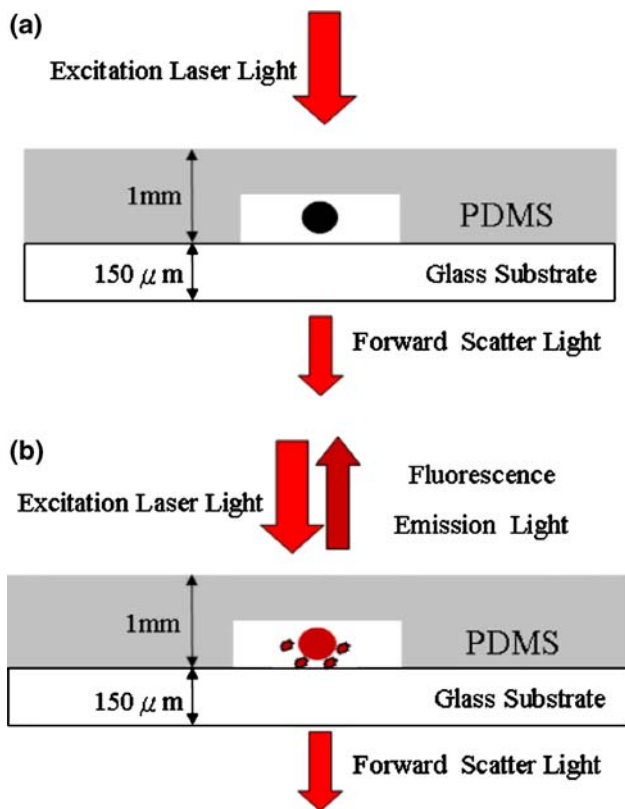


Fig. 2 Cross-sectional dimensions of the microchip and schematics diagram outlining principle of the detection system. **a** Forward scattered light paths for non-fluorescence particle detection. **b** Forward scattered light and backward fluorescence light paths for fluorescence particle detection

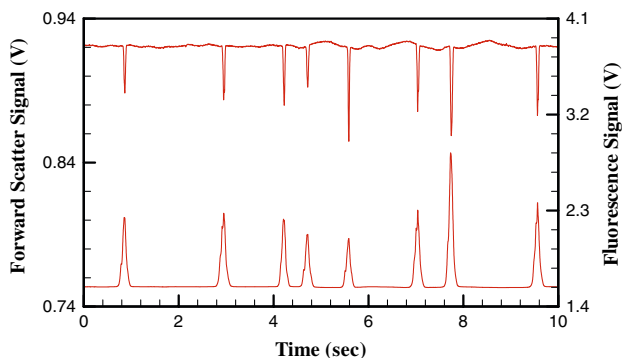


Fig. 3 Detection of forward light scattering and fluorescence signals for 100% labeled 10 μm particles. The upper plot and left axis indicates the forward scattered light signal; the lower plot and right axis indicates the fluorescence signal

the corresponding fluorescence detection signal are demonstrated in parallel when 100% ultra rainbow fluorescent particles of 10.2 μm diameter pass through the detection region. All the fluorescent particles pass through the detection region are recorded by the forward scattered light detector in size and the fluorescence detector in fluorescence intensity. The amplitude of each downward peak in

scattered light intensity indicates the size of particle and the corresponding upward peak in fluorescence intensity indicates the fluorescent emission of the particle. The present scattered signal detection technique employs the concept of resistive pulse sensing method because it can perform total counting by detecting all cells passing through the sensing channel (Wang et al. 2008). The one-to-one correspondence of the two types of signals shows that the scattered signal is highly synchronous with the fluorescence signal. It is different from the microfluidic image cytometry (Olsen and Adrian 2000; Hirono et al. 2008) using the acquired image information to determine the concentration of the particles in the suspension. However, the diameter of the scattering light detection fiber (50 μm in diameter) is only one-fourth of the fluorescence detection fiber (200 μm in diameter), the time period for a particle to pass the scatter light detection region is much shorter than that to pass the fluorescence detection region, and therefore scattered light signal response time (the width of the spikes) is shorter than fluorescence detection signal.

To determine the percentage of labeled particles in the suspension, the mixture of ultra rainbow fluorescent particles of 10.2 μm in diameter and non-fluorescence polystyrene particles of 9.86 μm in diameter were used in the experiments. Figure 4 shows the scattered light and fluorescent signals of above mixture of fluorescent and non-fluorescent particles. Two individual tests were conducted with each test of about 6 min, but only a segment of 120 s is presented in Fig. 4. From the result, we can justify exactly which particles are fluorescent labeled and the percentage of the labeled particles to the total count. The sample particle whose population of each run is 202 and 351 corresponding labeled particle number is 132 and 212. The percentage of the labeled particles in the individual test is 65.4 and 60.4%, respectively. As shown in Fig. 4, the fluorescence optical signals of 10 μm particle are more uniform in amplitude than the forward scattered intensity. One of the possible reasons is the particles always pass through the central region of the fluorescence detection fiber via passive focusing, which is achieved by shrinking the channel width from 200 to 50 μm. The convergent channel squeezes all the particles into a very thin stream passing through the fluorescent detection region of 200 μm in diameter. However, the 50 μm diameter barely matches the width of the convergent channel. Therefore, not all the incoming particles are aligned with the central region of the detection fiber. If a particle travels through the detection circle close to the circular edge, the scattered light intensity may be much weaker. The other one is the non-uniform size distribution of non-fluorescence particles in the range of 8.1–12 μm. The wide particle size distribution causes non-uniform scattered light intensity signals.

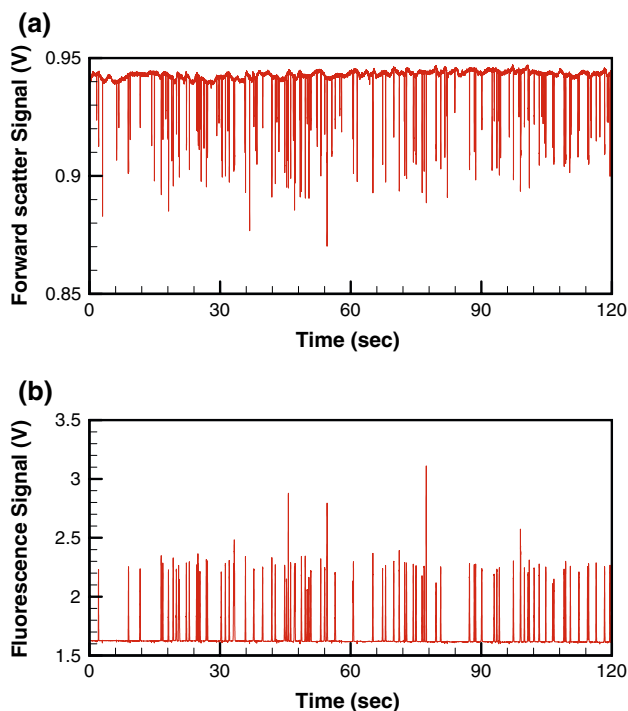


Fig. 4 Detection of forward scattered light signals and correspondence of fluorescence signals for a mixture of 10.2 μm labeled and 9.86 μm unlabeled particle. **a** Forward scattered light signal, **b** the corresponding fluorescence signal

Figure 5 shows optical signals of mixed ultra rainbow fluorescent particles of 10.2 μm in diameter and non-fluorescence polystyrene particles of 6 μm in diameter. Both scattered and fluorescence light signals are induced when 10.2 μm fluorescence particles pass through the detection region. However, only individual scattered signal is induced when the 6 μm unlabeled particles pass through. Assume that the particles pass through the center of the detection area, the intensity of forward light scattering is

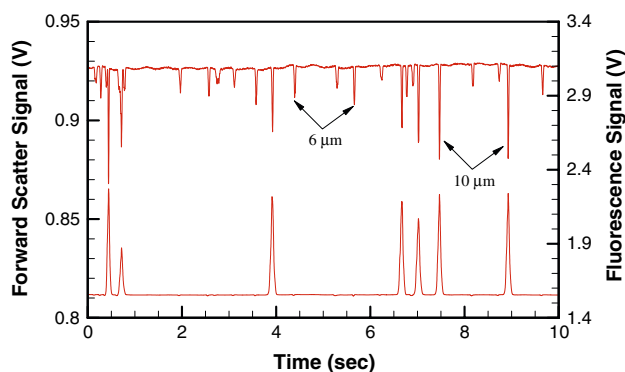


Fig. 5 Detection of forward scattered light and fluorescence signals for a mixture of 10.2 μm labeled particles and 6 μm unlabeled particle. The upper plot and left axis indicates the forward scattered light signal; the lower plot and right axis indicates the fluorescence signal

proportional to the size of particle. Therefore, the 10.2 μm particles have higher forward scattered light intensity when compared with the 6 μm particles. The observations are consistent with that for forward angle Mie scattering intensity which is proportional to the particle surface area or the square of the particle diameter.

To explore the capability of the proposed device for discrimination of different sized particles, four different diameters of 3, 4.8, 6 and 10.2 μm forward scattered signals of the particles were measured individually. The experimental results of four different diameter polystyrene particles size histogram analysis are shown in Fig. 6. The data show histograms of the number events as a function of forward scattered light intensity and Gaussian distribution. The amplitude of the light scattering intensity is measured in the low angle forward direction from the illuminating laser beam that is strongly influenced by the particle size. The four different groups of particles can be distinguished from the distribution histogram of the forward scattered light intensity. According to the data and statistical analysis, the statistical mean of the forward scattered light intensity of the four groups of particles are 4.36, 9.29, 14, 37.65 mV and the standard deviations are 1.32, 2.9, 3.53, and 11.23 mV, respectively. The coefficient of variation (CV) is a normalized measure of dispersion of distribution defined as the ratio of standard deviation to mean of the signal intensity. The CVs of four groups of particles are 30.2, 31.2, 25 and 29.8%, respectively. According to Mie's scattering theory, the intensity of scattered light is inversely proportional to the square of the distance from the particle to the observation point. In the experiment, the particle motion is limited by the height 30 μm of the microchannel, and the scattering light detection fiber is fixed underneath and in close contact with the glass substrate. Thus, the distance from the particle to the observation point could be minimized, and the highest scattered light intensity could be obtained in this configuration of the proposed device. On the basis of the experimental results, the CV percentage in the range of 25–31% agrees well with the test results reported by the other researchers (Pamme et al. 2003; Wang et al. 2004) which are in the range of 25–30% from a microfluidic device using the laser light scattering technology with photomultiplier tube systems for latex particle sizing.

To verify the forward scattered signal amplitudes relationship of monodisperse particle of different sizes, Fig. 7 shows the linear regression relativity of light scattered intensity for particles of four different sizes. The experimental results were obtained from the mean of particle scattered light amplitude. The result shows that the forward scattered light intensity is a fine linearity characteristic proportional to the various particle size. As mentioned earlier, the CV for the scattered light data is higher than

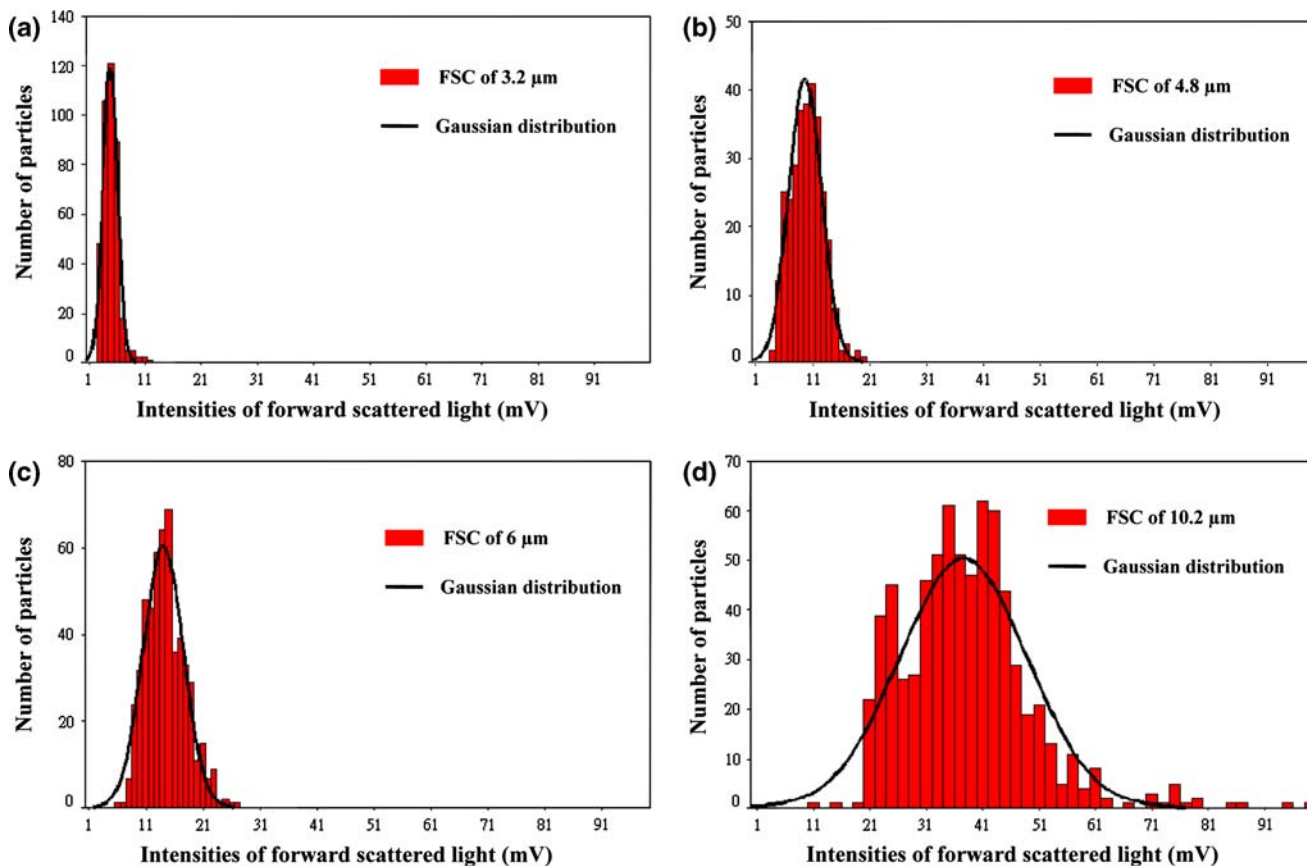


Fig. 6 Distributions of forward scattered light amplitude analysis for four different size polystyrene particles; **a** 3.2, **b** 4.8, **c** 6 and **d** 10.2 μm in the mean diameter

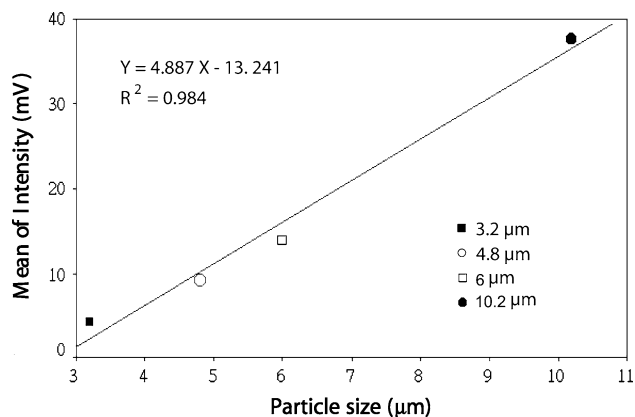


Fig. 7 Linear fits of the mean forward scattered light intensity for different size particles

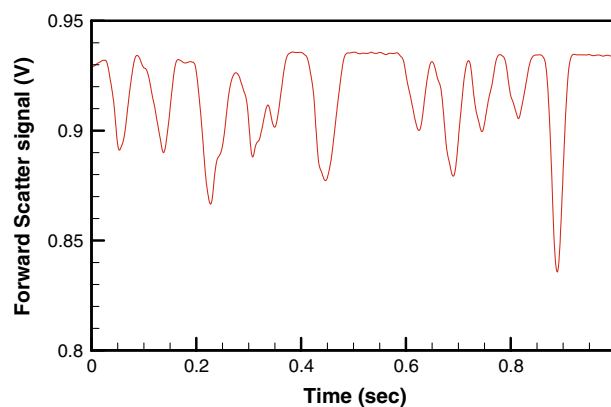


Fig. 8 High-throughput analysis by 10.2 μm forward scattered signals

that by a commercial flow cytometer. However, this problem can be solved by active hydrodynamic focusing to decrease the CV percentage.

Throughput is one of the important performance indexes of a flow cytometer, i.e., how many cells/particles can be analyzed for a specific time period. The faster counting speed, the more samples can be analyzed and the lower unit

cost for each test. To evaluate the efficiency of the proposed microflow cytometer, a fiber of 50 μm diameter was utilized for particles scattered light detection. As shown in Fig. 8, a counting rate of 11 particles per second was achieved in the scattered light signals. Each downward peak indicates a particle passing through the detection region. It can be observed that there are still some overlap

spikes, which could be minimized by further shortening the detection fiber to a size comparable to the cell diameter. It is expected that the proposed device can achieve a throughput comparable to the current commercial flow cytometers. The microchip device incorporates external optical components for on-chip sensing. By doing so, the internal transportation buffer disturbance and the electronic sensing components interconnected in a microchip can be eliminated. Surely, the system noise can be effectively reduced and the signal to noise ratio eventually enhanced.

Furthermore, flow rate is another factor to determine the performance of a microflow cytometer. The increased flow rate can improve the device throughput significantly. Generally speaking, electroosmotic flow and pressure-driven flow are two major types of methods for sample transport in the lab-on-a-chip device. Both of the transport methods can be used in our proposed device. Electroosmotic flow was applied to this study for sample transport, and a counting rate of 11 particles per second was achieved. It is noted that the throughput is low under-electrokinetic transport method. However, this article is a proof of concept investigation that demonstrates the effectiveness of the proposed method. Further effort to optimize the device performance and increase the system throughput is desired in the future. As an alternative approach, pressure-driven flow by integrating syringe pump can be applied to increase significantly the flow rate and hence the throughput of the detection system.

4 Summary

This study has presented a novel multi-functional optical flow cytometer that can perform particle counting, sizing and fluorescence detection on a microchip. An external fiber-to-fiber alignment for the optical microflow cytometer has been achieved in the experiment. Forward scatter was measured along the axis of the laser beam and backward fluorescence was measured by the laser excitation fiber. The fluorescence and size information of particle were characterized by combining these two types of signals. The experimental results not only show the total count of particles and relative percentage of labeled particles but also distinguish the different particle sizes based on forward scattered light intensity. In the proposed scheme, the optical microflow cytometer was fabricated with single-layer PDMS structure by soft lithography protocol without slow and expensive processes such as substrate etching, fiber etching, and fiber mounting and alignment. Moreover, the external detection fiber barely contacts the surface of microchip in the detection processes. The detection fibers can be reused because of the reduced abrasion, which significantly simplifies the

fabrication process and reduces the fabrication cost. This optical detection configuration utilizes external optical components for on-chip sensing that eliminates the disturbance to the internal buffer transportation and reduces system noise. Overall, an on-chip multi-functional optical flow cytometer is demonstrated to be highly reliable in particle analysis and can be a useful tool in application of lab-on-chip cellular analysis.

Acknowledgments The authors appreciate Professor Dongqing Li of the Department of Mechanical Engineering in Vanderbilt University for providing experimental facilities and valuable discussions.

References

- Ateya DA, Erickson JS, Howell PB Jr, Hilliard LR, Golden JP, Ligler FS (2008) The good, the bad, the tiny: a review of microflow cytometry. *Anal Bioanal Chem*. doi:10.1007/S00216-007-1827-5
- Bernini R, Nuccio ED, Brescia F, Minardo A, Zeni L, Sarro PM, Palumbo R, Scarfi MR (2006) Development and characterization of integrated silicon micro flow cytometer. *Anal Bioanal Chem* 386:1267–1272
- Cram LS (2002) Flow cytometry: an overview. *Method Cell Sci* 24:1–9
- Carbonaro A, Sohn L (2005) A resistance-pulse sensor chip for multianalyte immunoassays. *Lab Chip* 5:1155–1160
- Chen H-T, Wang Y-N (2008) Fluorescence detection in a micro flow cytometer without on-chip fibers. *Microfluid Nanofluid* (in press). doi:10.1007/S10404-008-0305-5
- Cheung K, Gaward S, Renaud P (2005) Impedance spectroscopy flow cytometry: on-chip label-free cell differentiation. *Cytometry A* 65:124–132
- Cui L, Zhang T, Morgan H (2002) Optical particle detection integrated in a dielectrophoretic lab-on-a-chip. *J Micromech Microeng* 12:7–12
- Dittrich PS, Schuille P (2003) An integrated microfluidic system for reaction, high-sensitivity detection, and sorting of fluorescent cells and particles. *Anal Chem* 75:5767–5774
- Erickson D, Li D (2004) Integrated microfluidic devices. *Anal Chim Acta* 507:11–26
- Fu L-M, Yang R-J, Lin C-H, Pan Y-J, Lee G-B (2004) Electrokinetically driven micro flow cytometers with integrated fiber optics for on-line cell/particle detection. *Anal Chim Acta* 507:163–169
- Fu L-M, Tsai C-H, Lin C-H (2008) A high-discrimination microflow cytometer with microweir structure. *Electrophoresis* 29:1874–1880
- Haynes John L (1988) Principle of flow cytometry. *Cytometry Suppl* 3:7–17
- Hirono T, Arimoto H, Okawa S, Yamada Y (2008) Microfluidic image cytometry for measuring the number and sizes of biological cells flowing through a microchannel using micro-PIV technique. *Meas Sci Technol* 19(025401):1–13
- Huh D, Tung Y-C, Wei H-H, Grothberg JB, Zhang M, Skerlos SJ, Kurabayashi K, Takayama S (2002) Use of air-liquid two-phase flow in hydrophobic microfluidic channels for disposable flow cytometers. *Biomed Microdevices* 4(2):141–149
- Huh D, Gu W, Kamotani Y, Grothberg JB, Takayama S (2005) Microfluidics for flow cytometric analysis of cells and particles. *Physiol Meas* 26:R73–R98
- Jagtiani AV, Zhe J, Hu J, Carletta J (2006) Detection and counting of micro-scale particles and pollen using a multi-aperture Coulter counter. *Meas Sci Technol* 17:1706–1714

- Knittle JE, Roach D, Vander Horn PB, Voss KO (2007) Laser-induced fluorescence detector for capillary-based isoelectric immunoblot assay. *Anal Chem* 79(24):9478–9483
- Luo C, Fu Q, Li H, Xu L, Sun M, Ouyang Q, Chen Y, Ji H (2005) PDMS microfluidic device for optical detection of protein immunoassay using gold nanoparticles. *Lab Chip* 5:726–729
- McClain MA, Culbertson CT, Jacobson SC, Ramsey JM (2001) Flow cytometry of *Escherichia coli* on microfluidic devices. *Anal Chem* 73:5334–5338
- Mogensen KB, Klank H, Kutter JP (2004) Recent developments in detection for microfluidic systems. *Electrophoresis* 25:3498–3512
- Morgan H, Holmes D, Green NG (2006) High speed simultaneous single particle impedance and fluorescence analysis on a chip. *Curr Appl Phys* 6:367–370
- Olsen MG, Adrian RJ (2000) Out-of-focus effects on particle image visibility and correlation in microscopic particle image velocimetry. *Exp Fluids* 29:S166–S174
- Pamme N, Koyama R, Manz A (2003) Counting and sizing of particle agglomerates in a microfluidic device using laser light scattering: application to a particle-enhanced immunoassay. *Lab Chip* 3:187–192
- Rodriguez-Trujillo R, Mills C, Samitier J, Gomila G (2007) Low cost micro-coulter counter with hydrodynamic focusing. *Microfluid Nanofluid* 3:171–176
- Saleh OA, Sohn LL (2003a) An artificial nanopore for molecular sensing. *Nano Lett* 3:37–38
- Saleh OA, Sohn LL (2003b) Direct detection of antibody–antigen binding using an on-chip artificial pore. *PNAS* 100:820–824
- Sun T, Holmes D, Gawad S, Green NG, Morgan H (2007) High speed multi-frequency impedance analysis of single particles in a microfluidic cytometer using maximum length sequences. *Lab Chip* 7:1034–1040
- Tung Y-C, Zhang M, Lin C-T, Kurabayashi K, Skerlos SJ (2004) PDMS-based opto-fluidic micro flow cytometer with two-color, multi-angle fluorescence detection capability using PIN photodiodes. *Sens Actuators B* 98:356–367
- Wang Z, El-Ali J, Englund M, Gotsaed T, Perch-Nielsen IR, Mogensen KB, Snakenborg D, Kutter JP, Wolff A (2004) Measurements of scattered light on a microchip flow cytometer with integrated polymer based optical elements. *Lab Chip* 4:372–377
- Wang Y-N, Kang Y, Xu D, Chon CH, Barnett L, Kalams SA, Li D, Li D (2008) On-chip counting the number and the percentage of CD4+ T lymphocytes. *Lab Chip* 8:309–315
- Wharton JE, Jin P, Sexton LT, Horne LP, Sherrill SA, Mino WK, Martin CR (2007) A method for reproducibly preparing synthetic nanopores for resistance-pulse biosensors. *Small* 3(8):1424–1430
- Xiang Q, Xuan X, Xu B, Li D (2005) Multi-functional particle detection with embedded optical fibers in poly(dimethylsiloxane) chip. *Instrum Sci Technol* 33:597–607
- Xu D, Kang Y, Sridhar M, Hmelo AB, Feldman LC, Li D, Li D (2007) Wide-spectrum ultrasensitive fluidic sensors with amplification from both fluidic circuits and metal oxide semiconductor field effect transistors. *Appl Phys Lett* 91:013901
- Yao B, Luo G-A, Feng X, Wang W, Chen L-X, Wang Y-M (2004) A microfluidic device based on gravity and electric force driving for flow cytometry and fluorescence activated cell sorting. *Lab Chip* 4:603–607
- Yi C, Zhang Q, Li C-W, Yang J, Zhao J, Yang M (2006) Optical and electrochemical detection techniques for cell-based microfluidic systems. *Anal Bioanal Chem* 384:1259–1268
- Zhe J, Jagtiani A, Prashanta Dutta, Hu J, Joan C (2007) A micromachined high throughput Coulter counter for bioparticle detection and counting. *J Micromech Microeng* 17:304–313